# We are IntechOpen,
# the world's leading publisher of
# Open Access books
# Built by scientists, for scientists

## 6,900
Open access books available

## 186,000
International authors and editors

## 200M
Downloads

## 154
Countries delivered to

Our authors are among the

## TOP 1%
most cited scientists

## 12.2%
Contributors from top 500 universities

**CLARIVATE ANALYTICS**
**BOOK CITATION INDEX**
**INDEXED**

**WEB OF SCIENCE**™

Selection of our books indexed in the Book Citation Index
in Web of Science™ Core Collection (BKCI)

# Interested in publishing with us?
# Contact book.department@intechopen.com

Numbers displayed above are based on latest data collected.
For more information visit www.intechopen.com

# Development of High Efficiency Two-Phase Thermosyphons for Heat Recovery

Ignacio Carvajal-Mariscal, Florencio Sanchez-Silva and Georgiy Polupan
*National Polytechnic Institute of Mexico*
*Mexico*

## 1. Introduction

Due to high fuel prices, it has become necessary to investigate new methods for saving and more efficient use of energy, emphasizing the use of energy remaining in the waste gases of combustion equipment. For this reason, in the last five decades there has been an important technological development in heat transfer equipment, to promote changes in configuration and applying heat transfer systems with high effectiveness. One example is the use of two-phase thermosyphons (Azada et al., 1985; Faghri, 1995; Gershuni et al., 2004; Noie, 2005; Peterson, 1994; Reay, 1981).

A two-phase thermosyphon is a device that is used for heat transfer; this process occurs inside it as a cycle of evaporation and condensation of a working fluid (Faghri, 1995; Peterson, 1994). This device is easily constructed, has no moving parts inside and works individually. The two-phase thermosyphon consists of: condensation, evaporation and adiabatic zones (Figure 1). Operation starts when heat is supplied to the evaporator zone, so a portion of the fluid evaporates, taking the latent heat of evaporation inside the tube up to the condenser section. In this last section, vapor condenses and transfers its latent heat of condensation to the surroundings. The condensate runs down as a film on the inner wall of the tube with the aid of gravity.

There have been conducted several investigations in the field of thermosyphon design and development. The authors of reference (Park et al., 2002) studied the heat transfer characteristics depending on the amount of working fluid and when the operation limits occur. The two-phase element was made of copper and as working fluid FC-72 (C14 F14) was used. The thermosyphon was subjected to a heat supply in the range of 50-600 W and with 10-70% load rate. For the convection coefficients in the condenser and in the evaporator, the authors used the theory of Nusselt and Roshenow respectively. They found that the operation limits manifest in different forms depending on the loading rate of the fluid. For small loading rates ($\Psi = 10\%$) the drying limit occurs in the evaporator, while for high loading rates ($\Psi = 50\%$) is the flooding limit that appears. In the first case, evaporator temperature increases from the evaporator bottom; in the second case the evaporator temperature increases at the top of the evaporator. These conclusions were made by observing the temperature distribution along the thermosyphon. Moreover, (Zuo & Faghri, 2002) conducted an analytical and experimental research on the thermodynamic behavior of the working fluid in a thermosyphon and a heat pipe, using a temperature-entropy diagram.
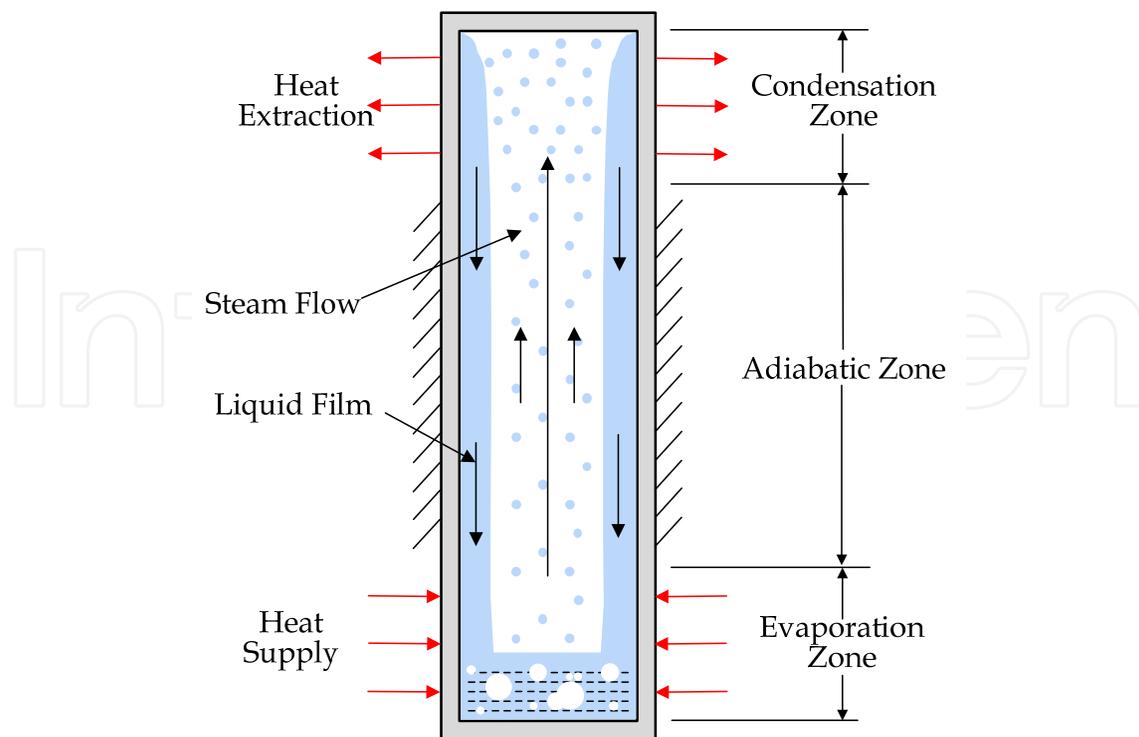
Fig. 1. Two-phase thermosyphon.

The authors divide the thermodynamic processes in 2 categories: 1) heat transfer by conduction through the tube wall and 2) heat and mass transfer, by convection inside the two-phase thermosyphon. (Noie, 2005) presented in his work an experimental study of a thermosyphon (980 mm of length and an internal diameter of 25 mm) made of copper and smooth inside, using distilled water as a working fluid. The goal of the study was to obtain the thermal characteristics of the thermosyphon (temperature distribution in the outer wall and all along the tube, boiling heat transfer coefficient and the maximum heat transfer rate), varying 3 parameters: heat supply ($100 < Q < 900$ W), loading rate ($30\% \leq \Psi \leq 90\%$) and length of the evaporator (varying the length of electrical resistance).

From above mentioned, it follows that in order to design high efficiency heat recovery equipment based on two-phase thermosyphons, there should be solved first the main issues inherent to to their manufacture: loading rate, maximum heat transfer rate, and compatibility between material of container and the working fluid. In order to address these issues, an analytical-experimental investigation has been carried out in the Thermal Engineering and Applied Hydraulics Laboratory, for the last four years. Following are presented the results of this investigation.

## 2. Design and manufacture

The design and manufacture of a thermosyphon is a complex process because there should be considered several parameters such as length, shape, weight and volume of the device, heat load, transport distance, ratio of lengths between evaporator and condenser, acceptable temperature gradients, temperature range of operation, amount of working fluid, service life and safety. Of course, the working fluid thermophysical properties and the manufacturing material properties should be taken into account as key variables.

Because there are no standards in the public domain for the manufacture and design of two-phase thermosyphons is necessary to develop the methodologies to design them. Following are described three methodologies for the calculation of key parameters used in the design and manufacture of two-phase thermosyphons. For the development of these methodologies water was considered as the working fluid.

The first parameter to calculate is the relation between the lengths of the zones of evaporation and condensation, and the total length of the thermosyphon. From this relation it can be obtained the total length of the thermosyphon for certain heat recovery equipment.

For security reasons, one of the most important parameters to be calculated is the working pressure of thermosyphon under different operation conditions and for distinct amounts of working fluid in the thermosyphon. These working pressures of the internal fluid are: the pressure when the device is off, i.e., when the thermosyphon is at room temperature, this is when the device is in non-operating conditions (transportation, storage, etc.), and the operating pressure.

The third parameter is the evaporation rate of the working fluid in the process of loading the thermosyphon. This process is directly related to the procedure of loading the working fluid to the thermosyphon, which was implemented in this research.

### 2.1 Relations between the lengths of the areas of air and gases and the total length of the thermosyphon

Heat recovery equipment based on two phase thermosyphons consists of an outer envelope with thermosyphons grouped inside. According to the principle of operation of the thermosyphons (evaporation/condensation of a working fluid) heat is transferred from the evaporator, located at the bottom where the combustion hot gases flow, to the condenser, located at the top, where the fluid to be heated circulates. Thus, the hot gases flowing through the evaporation zone, transferring the heat from that zone to the condensation zone through the thermosyphons. On the other hand, the gases to be heated, for example air, flow in the opposite direction through the condensation zone absorbing the heat dissipated by the thermosyphons.

It can be considered that the efficiency of the thermosyphon is 95%, that is, 95% of heat of combustion gases is transferred into the condensation zone for heating the air. The energy balance for steady state conditions may be expressed as:

$$\dot{m}_a c_{pa}\left(T_{a,out} - T_{a,in}\right) = \dot{m}_g c_{pg}\left(T_{g,in} - T_{g,out}\right) \tag{1}$$

Applying the continuity equation gives the expression (2).

$$\rho_a A_a v_a c_{pa}\left(T_{a,out} - T_{a,in}\right) = \rho_g A_g v_g c_{pg}\left(T_{g,in} - T_{g,out}\right) \tag{2}$$

In addition, the area for the passage of air, $A_a$, is defined as the product of the length of the thermosyphon condensation zone, $l_c$, by the width of the passage of air, $a$:

$$A_a = l_c a \tag{3}$$
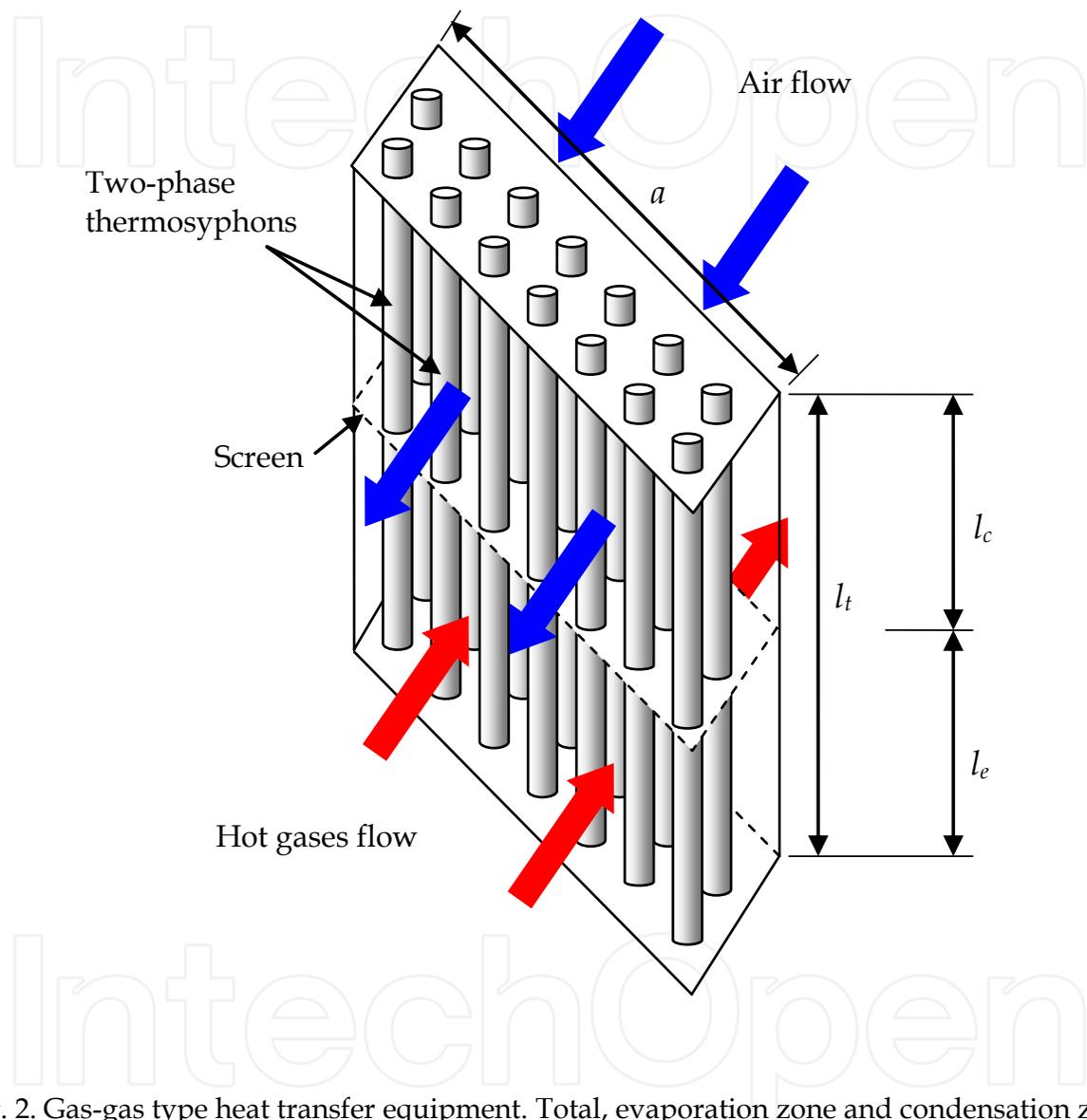
Fig. 2. Gas-gas type heat transfer equipment. Total, evaporation zone and condensation zone characteristic lengths are shown.

Similarly, for the passage of hot gases

$$A_g = l_e a \tag{4}$$

Because the adiabatic zone is negligible, the total length of the thermosyphon is the sum of the lengths of the evaporation and condensation zones (5),

$$l_t = l_c + l_e \tag{5}$$

This methodology considers that the velocities of hot gases and air are equal and that the thermosyphon has an efficiency of 95%. In addition, the width of the passage of air is equal to the width of the passage of hot gases, which is the width of the air preheater, *a*. Taking these considerations into account and substituting equations (3) and (4) in equation (2) gives the expression (6)

$$\rho_a l_c c_{pa}\left(T_{a,out} - T_{a,in}\right) = 0.95 \rho_g l_e c_{pg}\left(T_{g,in} - T_{g,out}\right) \tag{6}$$

To determine one of the design parameters sought, which is the ratio between the length of the condensation zone and the total length of the thermosyphon, equations (5) and (6) are resolved simultaneously and following equation (7) is obtained.

$$\frac{l_c}{l_t} = \frac{0.95 \rho_g c_{pg}\left(T_{g,in} - T_{g,out}\right)}{0.95 \rho_g c_{pg}\left(T_{g,in} - T_{g,out}\right) + \rho_a c_{pa}\left(T_{a,out} - T_{a,in}\right)} \tag{7}$$

Knowing this, from equation (5) is obtained the relation between the length of the evaporation zone and the total length of the thermosyphon (8).

$$\frac{l_e}{l_t} = 1 - \frac{l_c}{l_t} \tag{8}$$

However, the equations developed above, consider only the energy and mass balances, this analysis could lead to violations of the second law of thermodynamics. To be sure that the results do not violate this law, the mathematical models to calculate the entropy production in the system are used. Just for recalling that the total entropy change must be greater than or equal to zero.

If the air is considered as an ideal gas and the isobaric heating process is reversible, then the entropy change of air is expressed as follows:

$$\Delta \dot{S}_a = \dot{m}_a c_{pa} \ln\left(\frac{T_{a,out}}{T_{a,in}}\right) \tag{9}$$

Similarly for combustion gases the entropy change is expressed as follows:

$$\Delta \dot{S}_g = \dot{m}_g c_{pg} \ln\left(\frac{T_{g,out}}{T_{g,in}}\right) \tag{10}$$

The expression to calculate the total entropy change of the system is as follows:

$$\Delta \dot{S}_{sys} = \Delta \dot{S}_g + \Delta \dot{S}_a \tag{11}$$

As an example, a parametric analysis to study the relationship of the lengths of the zones of evaporation and condensation with respect to the total length of the thermosyphon was carried out. The outlet temperatures of both air and combustion gases were varied. The air inlet temperature is assumed to be 25 °C and the combustion gases of 250 °C. The

investigated interval of the air outlet temperature is 35 ºC to 105 °C. If temperature difference between the entrance and outlet of both air and gas are equal to 70 ºC,

$$T_{a,out} - T_{a,in} = T_{g,in} - T_{g,out} = 70 \text{ ºC} \qquad (12)$$

so at the exit of the air preheater, outlet temperatures of air and hot gases are equal to $T_{a,out}$ = 95 °C and $T_{g,out}$ = 180 °C. This requires that the ratios of the lengths of the zones must be 42% of $l_t$, as shown in Figure 3, and $l_e$ must be 58% of the total length of the thermosyphon according to the equations (7) and (8).

## 2.2 Operating pressure

To determine the pressure during operation and non-operation of the thermosyphons, there were considered the loading ratios, and ambient temperature and pressure at which was done the loading process of the thermosyphon. The loading ratio is determined by

$$\Psi = V_f / V_t \qquad (13)$$

After choosing the values of loading ratios, it can be obtained the working fluid volume; in this case is water, and therefore it may also be known the mass, $m_f$, of water that fills the thermosyphon. After the loading process of the thermosyphon, this mass of water, $m_f$, will fill the total internal volume of the thermosyphon, $V_t$, as steam and liquid, so the specific volume of water can be determined by the expression (14)

$$\upsilon_f = V_t / m_f \qquad (14)$$

Upon completion of loading process of the thermosyphon, it is then sealed and exposed again to ambient temperature, therefore, the internal pressure drops to the design parameter called the non-operating pressure. From the tables of thermodynamic properties of water (Incropera & Dewitt, 2006) the value of the non-operating pressure is determined with the values of ambient temperature, $T_{amb}$, and the specific volume, $\upsilon_f$.
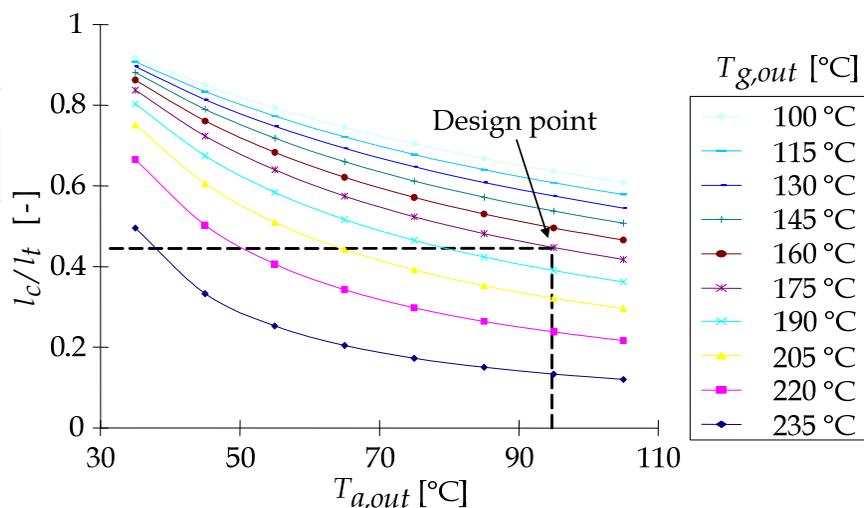


Fig. 3. Length of the condensation zone and total length versus the outlet air temperature, for different outlet temperatures of gases.

The operating pressure of the thermosyphon is also found in the tables of thermodynamic properties of water (Incropera & Dewitt, 2006), the specific volume of water was calculated with the equation (14), $\upsilon_f$, and operating temperature.

To calculate the operating pressure of the thermosyphon a parametric analysis was performed, where the variable parameter is the loading ratio. The interval of studied loading ratio is 5% to 45%. The geometric characteristics of the thermosyphon were taken as follows: length of 1 m and a diameter of 2.54 cm. The temperature of 20 °C and a pressure of 1 bar were the ambient conditions. It was considered that the maximum operating temperature of the thermosyphon is 250 °C.
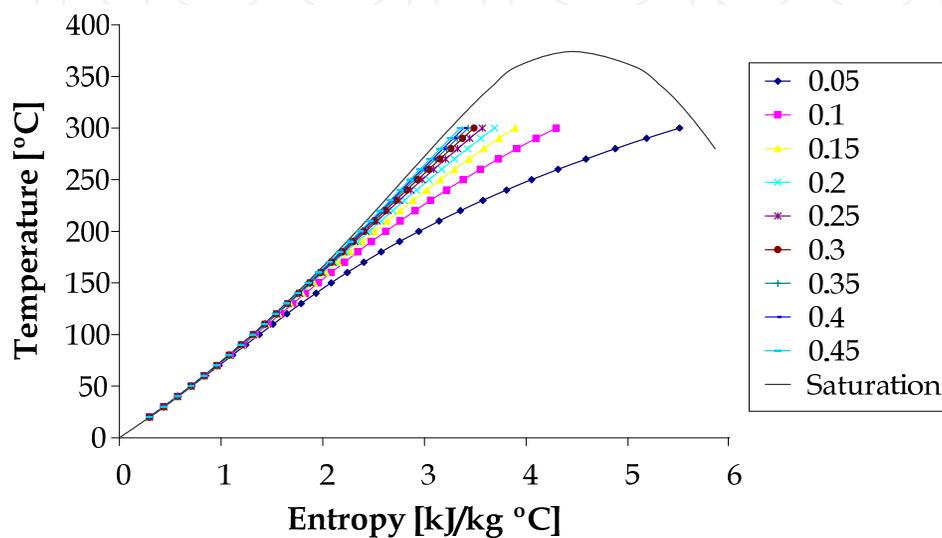


Fig. 4. T-s diagram of isochoric operation of the thermosyphon for different loading ratios.

Figure 4 shows in a T-s diagram the isochoric process that takes place in the thermosyphon for different loading ratios, from 5% to 45%.

As an example applying the described method a loading ratio of 10% is given, and the value of the specific volume of water that was obtained using equation (14) is 0.0100177 m³/kg. Therefore by exposing the thermosyphon at room temperature of 20 °C, after the loading process, the non-operating pressure is equal to 0.0233 bar. Table 1 shows the thermodynamic properties of water inside the thermosyphon. On the other hand, by bringing the thermosyphon to the operating temperature for an isochoric process, an operating pressure equal to 39.7 bar is achieved. Table 1 shows the properties for the operating temperature of 250 °C and the specific volume of 0.0100177 m³/kg.

| $T$ (°C) | $p$ (bar) | $\upsilon$ (m³/kg) | $H$ kJ/kg | $s$ kJ/kg °C | $x$ (-) | $u$ kJ/kg | $c$ kJ/kg °C |
|---|---|---|---|---|---|---|---|
| 20 | 0.0233 | 0.010017 | 84.21 | 0.297 | 0.00015 | 84.83 | 5.8805 |
| 250 | 39.7 | 0.010017 | 1393.1 | 3.38 | 0.1794 | 1353.3 | 238.0 |

Table 1. Properties of the working fluid, water, for 10% loading ratio and non-operating conditions.

### 2.3 Evaporation rate

In the loading procedure developed in this research it is required that part of the working fluid evaporates filling all the internal volume of the device and forcing the non condensable gases to leave from the upper end of the thermosyphon. Thus, in this process a small amount of water escapes, so the initial water mass must be bigger than the desired final mass inside the thermosyphon. Therefore, it is important to determine the time of evaporation of the desired amount of initial fluid. This methodology proposes to know this time by the rate of evaporation or mass flow rate of evaporation from a free water surface (Incropera & Dewitt, 2006), defined by the following equation

$$\dot{m}_{eva} = \bar{h}_m A_{eva} \left( \rho_{v,satop} - \phi \rho_{v,satam} \right) \tag{15}$$

In the tables of saturated water vapor (Incropera & Dewitt, 2006), it was obtained the saturation density corresponding to room temperature, $\rho_{v,satam}$, and the saturation density corresponding to the temperature of the fluid during the loading process, $\rho_{v,satop}$.

The area of evaporation surface, $A_{eva}$, can be obtained from the following expression

$$A_{eva} = \pi d_{int}^2 / 4 \tag{16}$$

To calculate the mass transfer coefficient ($\bar{h}_m$) it was used the analogy of heat and mass transfer (Incropera & Dewitt, 2006)

$$\bar{h}_m = \bar{h}_a / \left( \rho_a c_{pa} \right) \left( D_{a,w} / \alpha_a \right)^{2/3} \tag{17}$$

The binary diffusion coefficient is calculated using the following relation

$$D = D_0 \left( p_0 / p \right) \left( T / T_0 \right)^{3/2} \tag{18}$$

To calculate the average coefficient of free convection it was used the definition of Nusselt number, equation (19) (Incropera & Dewitt, 2006)

$$\bar{h}_a = k_a \, \mathrm{Nu} / L_{eva} \tag{19}$$

Where the Nusselt number is given by equation (20) for Rayleigh numbers, Ra ≤ 109 (Incropera & Dewitt, 2006)

$$\mathrm{Nu} = 0.68 + \frac{0.67 \, \mathrm{Ra}^{1/4}}{\left[ 1 + \left( 0.492 / \mathrm{Pr} \right)^{9/16} \right]^{4/6}} \tag{20}$$

Where the Rayleigh number is defined by equation (21) (Incropera & Dewitt, 2006)

$$\mathrm{Ra} = \mathrm{Gr} \times \mathrm{Pr} \tag{21}$$

Where the Grashof number, Gr, which is the ratio between buoyancy forces and viscous, is defined by the expression (21) (Incropera & Dewitt, 2006)

$$Gr = g\beta_a T_p L_{eva}^3 \Big/ v_a^2 \tag{22}$$

From the tables of properties of air, it is possible to get all the properties required to find the values of the parameters above mentioned using the average air temperature, $T_p$ (23). This average temperature is obtained from room temperature, $T_{amb}$, and temperature of the thermosyphon during the loading process, $T_{op}$.

$$T_p = \frac{\left(T_{amb} + T_{op}\right)}{2} \tag{23}$$

The developed methodology allows the calculation of the evaporation rate to analytically study the behavior of the flow of water evaporation as a function of ambient conditions that occur at the time of the loading process of the thermosyphon.

A parametric analysis was made with the same geometric conditions that the above described analysis, it is considered a thermosyphon with a length of 0.9 m and an inner diameter of 2.15 cm. The ambient conditions were taken as 20 °C and a pressure of 1 atm. The temperature of the thermosyphon during the filling process, $T_{op}$, which takes place during the loading process is 100 °C. The characteristic length of evaporation, $L_{eva}$, is equal to the area divided by the perimeter of the orifice where the steam escapes from the thermosyphon during the filling process.

Figure 5 shows the evaporation mass flow as a function of the temperature for different relative humidity, ranging from 40% to 90%.
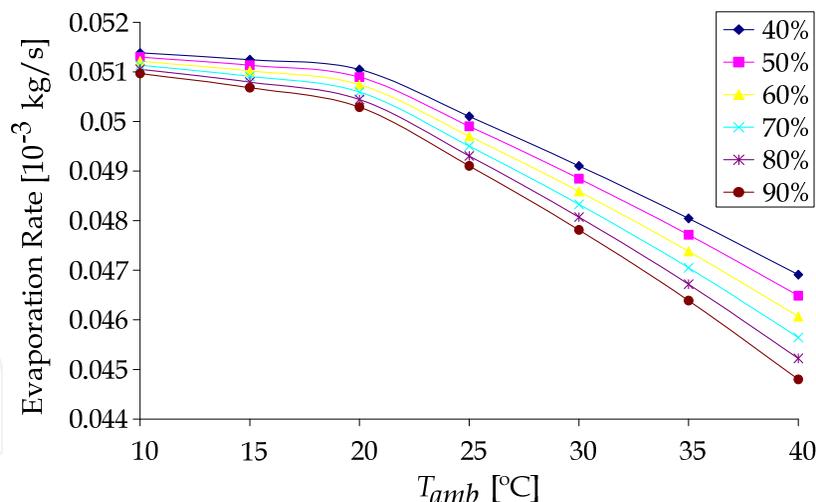


Fig. 5. Evaporation mass flow as a function of the ambient temperature and relative humidity.

## 2.4 Control of corrosion in the thermosyphons

The use of steel and water as a building material and working fluid, respectively, is very attractive in the design of the thermosyphon due to its low cost and high heat transmission (Terdtoon et al. 2001). However, it is well known that the ferrous material is chemically incompatible with water, and a manifestation of this incompatibility is the appearance of

rust. To avoid this effect, there have been used a series of corrosion-inhibiting additives that are added to water, among which is hydrazine hydrate.

For application in thermosyphon tubes, hydrazine hydrate has the following characteristics:

- It is dosed at a ratio close to 1:1 for the concentration of dissolved oxygen in water.
- In the form of hydrazine hydrate is considerably reduced the toxicity of pure hydrazine.
- Generates no solid waste.
- Pressure and temperature of degradation are higher than those to be taken when operating the thermosyphon in heat recovery processes of medium temperature (up to 300 ºC).
- Acts as a passivator by forming a protective layer.

Hydrazine interacts with the iron oxide to form magnetic iron oxide $Fe_3O_4$ (magnetite), which is of black color and usually forms in water or steam when there is a deficiency of oxygen and on a layer of $Fe_2O_3$ (hematite). This film or barrier that adheres to the metal surface prevents the transport of reactive species of water, or the transport of products outside of this interface, i.e., prevents the flow of electricity. Therefore, the metal-water system is not oxidized or reduced, so the addition of hydrazine can slow and sometimes halt the destruction of the steel.

The addition of hydrazine hydrate to thermosyphon working fluid may have some effect on the heat transfer of the device. Therefore, it was determined experimentally the influence of the amount of hydrazine hydrate on the thermal performance of a thermosyphon. The results of this research are presented in (Carvajal-Mariscal et al., 2011) and it was found that the minimum concentration of hydrazine hydrate, which is necessary to reduce the effects of corrosion, but little changes the thermal performance of the thermosyphon is 50 mg/L.

## 2.5 Manufacture of the two-phase thermosyphon

The two-phase thermosyphons used in this investigation were made with A179 carbon steel tubes, with 900 mm long, 25.4 mm external diameter and 21.5 mm inner diameter. According to the calculations using the methodology above mentioned and corrected to standard sizes, was established that the length of the condensation zone should be 40% of the length of the thermosyphon, and the other 60% is the evaporation zone. Because it was chosen the length of the thermosyphon equal to 90 cm, so the evaporation zone has a length of 0.55 m and the length of the condenser is 0.35 m.

Generally, the thermosyphons are built with a lid of the container of the same material at the bottom which is welded to the container. At the top is also welded a cap, which has a concentric orifice where is welded an appendix, which is used to enter the working fluid, and also serves to facilitate the sealing. However, the thermosyphons used in this study were constructed with the following additions: The lower end is fitted with a coupling to use a tapered cap of 3/8 of diameter and with a PTN thread. At the top is installed a needle valve.

Coupling was implemented at the bottom because its diameter allowed the cleaning and loading of the working fluid, the conical cap was chosen to avoid leaks of the working fluid during the testing. The needle type valve was implemented for quick and easy sealing of the

thermosyphons. This avoids the use of a complex procedure that could cause leakage or contamination inside the thermosyphon.

It was also determined that the material of which has to be built the core of the thermosyphon is A-179 carbon steel. This type of material is commercial steel used in the manufacture of heat exchangers and boilers. In order to check if the wall thickness is adequate, i.e., if the tube will withstand the maximal operating pressures, it was used the equation (24)

$$t = \frac{p_i r_{ext}}{\zeta E + 0.4 p_i} = \frac{(40 \, \text{bar})(0.0127 \, \text{m})}{\left[(1800 \, \text{bar})0.85 + 0.4(40 \, \text{bar})\right]} = 0.341 \, \text{mm} \tag{24}$$

It was obtained a minimum thickness of 0.341 mm, which is less than the thickness of the commercial tube (1.953 mm) used in the thermosyphons, so it is guaranteed to use it only to the pressures and temperatures planned in this investigation, without the risk of an accident.

The chosen working fluid is distilled water. Distilled water was chosen because of its easy availability, is not dangerous and its thermodynamic and physical properties are well known, also allows the use of the thermosyphon in the range of 5 °C to 250 °C.

Table 2 presents the specifications of the thermosyphon designed and implemented in this investigation.

| | |
|---|---|
| Total length | 900 mm. |
| Evaporator length | 525 mm. |
| Adiabatic zone length | 25 mm |
| Condenser length | 350 mm. |
| Inside diameter of the container | 21.5mm |
| Outside diameter of the container | 25.4 mm |
| Outer diameter of aluminum tube | 27 mm |
| Fin diameter | 53.9 mm |
| Material of the container | Carbon Steel A-179. |
| Material of the outer tube and fins | Extruded aluminum |
| Working fluid | Distilled water |
| Maximum operating pressure | 40 bar |
| Maximum operating temperature | 250 ºC |

Table 2. Specifications of the two-phase thermosyphons.

## 3. Experimental investigation

The aim of experimental research is to understand the performance of a thermosyphon when varying the following parameters: amount of working fluid, heat supply and cooling air speed. To achieve this there were designed two experimental facilities for loading the working fluid and for testing the efficiency of two-phase thermosyphon.

### 3.1 Installation for loading of working fluid

Figure 6 shows an outline of the facility for loading working fluid. It consists of an array of 2 resistors of the band type with an electrical power of 250 W each. The supply of electricity to the resistance was provided by a voltage variable autotransformer of 1.4 kW and power was calculated from data obtained by a voltmeter and an ammeter, both digital.

Before starting the loading procedure of fluid inside the thermosyphon, the tube was cleaned with soapy water and rinse with distilled water followed by methyl alcohol and finally dried by applying heat. After that the process of loading fluid began.

First to fill the thermosyphons with the required filling rate, it must be known how quickly the fluid evaporates in the loading process. To carry out this process a known mass of water was introduced, then the evaporator section was heated and some time was allowed to evaporate this water mass.

In this research seven tests of loading were performed at different times. The testing time was measured when the steam started to leave the thermosyphon from the needle valve installed on the top, until closing the valve. After valve was closed and the device was cooled off, the working fluid was removed to check how much fluid was ejected from thermosyphon during the loading process.

The loading process consisted of heating for some time the thermosyphon filled with a little more than the desired amount of fluid. This in order to evaporate the difference, and so fill all the volume with water vapor, so that it forces the non-condensable gases to escape through the needle valve installed on the top of the thermosyphon, along with water vapor excess. Knowing the rate of evaporation of the fluid, the loading process time depends on the amount of fluid is desired to leave inside the thermosyphon.
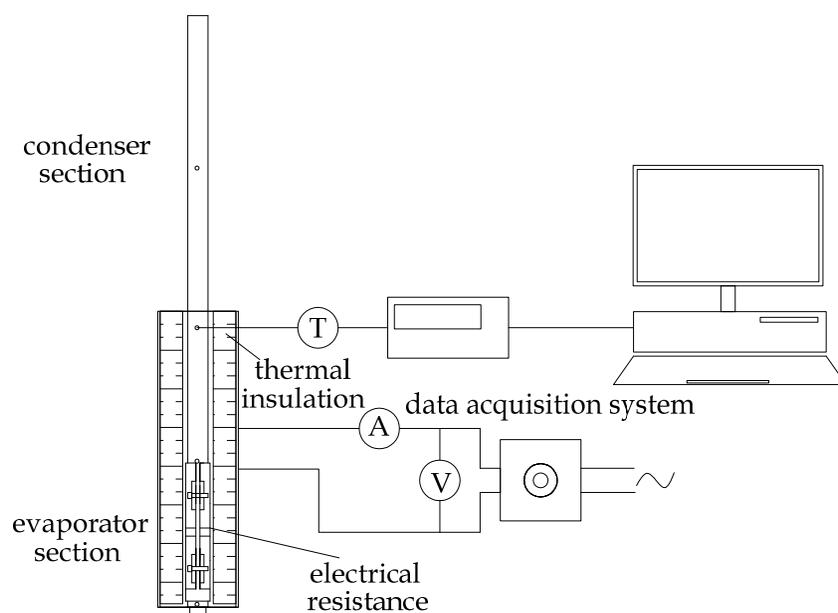


Fig. 6. Outline of the facility for loading working fluid.

To check the amount of fluid evacuated during the loading time, the steam was captured and taken through a condenser to a container where the mass ejected can be measured by a

scale. The electrical resistances arrangement of the evaporator was isolated with mineral wool and a stainless steel shell, in order to minimize heat losses.

With this method of loading the inner volume of the thermosyphon fills only with working fluid as vapor or liquid. This ensures that there are no non-condensable gases accumulated in it. The time that takes to perform this procedure depends on the excess fluid that has to be removed, in that way that at the end of the procedure only the desired amount of working fluid stays in the thermosyphon.

## 3.2 Testing facility for thermosyphon performance

Figure 7 shows a schematic of the experimental setup. It consists of a thermosyphon installed in a wind tunnel. On the section of the evaporator are placed, three electrical resistances of 250 W and 110 V AC. The power source is the same as in the previous installation.

Heat is removed from condenser section by a flow of cooling air. The test section is located on the suction side of the tunnel; the air is forced by an axial ventilator with a 1.12 kW motor. To measure the air temperatures at the inlet and outlet of the test section type "K" thermocouples were used. Moreover, seven K-type thermocouples were placed on the outer surface of the tube in order to measure the temperature distribution along the thermosyphon. The record of these temperatures was achieved by a Cole Parmer data acquisition system.
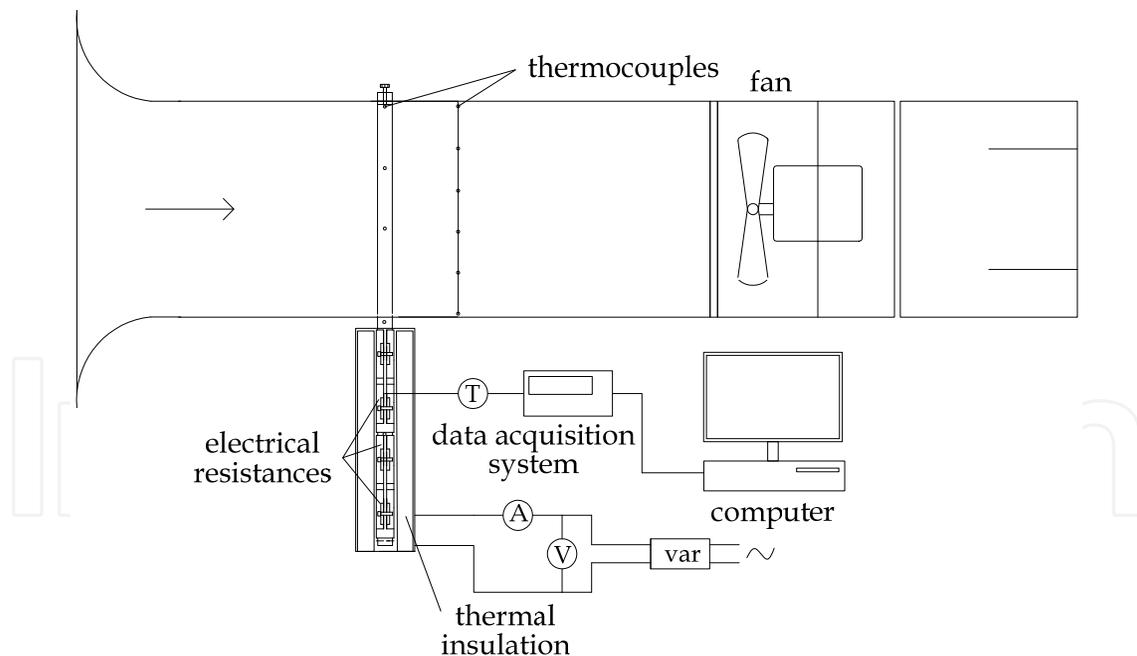


Fig. 7. Schematic of the experimental setup for thermosyphon performance testing.

Thermocouples were placed from the bottom of the evaporator in the positions of 5, 18, 35.5, 52, 65, 76.5 and 88 cm. These thermocouples were attached firmly to the surface and small sections of the fins were removed to provide a better placement.

The supply of heat to the evaporator section is calculated using the following relationship:

$$Q_{sup} = \frac{U^2}{R} = UI \tag{25}$$

On the other hand, the heat dissipated by the condenser is obtained by the following relationship:

$$Q_{ext} = \dot{m}_a c_{pa} \left( T_{out} - T_{in} \right) \tag{26}$$

The experimental tests consisted of the systematic variation of the supply of heat flow to the evaporator, keeping constant the amount of working fluid, the electric motor speed and the length of heating. Once the temperatures are stable throughout the thermosyphon this is considered a test point. Thus the data of temperature distribution and the heat dissipated is obtained for a loading volume of working fluid. Table 3 shows the parameters that were varied for these tests.

| Loading rates ($\Psi$) | 10%, 15%, 20%, 25%, 30% |
|---|---|
| Heat supply | 800 W < Q < 2000 W |
| Mass flow of cooling air | 0.175, 0.247, 0.380 kg/s |

Table 3. Test parameters.

## 4. Results and discussion

### 4.1 Thermosyphon behavior during loading of the working fluid

Figure 8 shows the time and mass of water leaved in thermosyphon after the loading tests applying 272 W to evaporate the fluid. By applying a least squares method to approximate the data it was obtained an evaporation rate equal to 3.2683 g/min. Figure 8 shows the line fitted to the data obtained experimentally, which has a negative slope. Table 4 presents the values of standard deviation in the final internal mass measurement and uncertainties in the estimated value of the interceptor and the value of the evaporation rate, calculated by the least squares method.
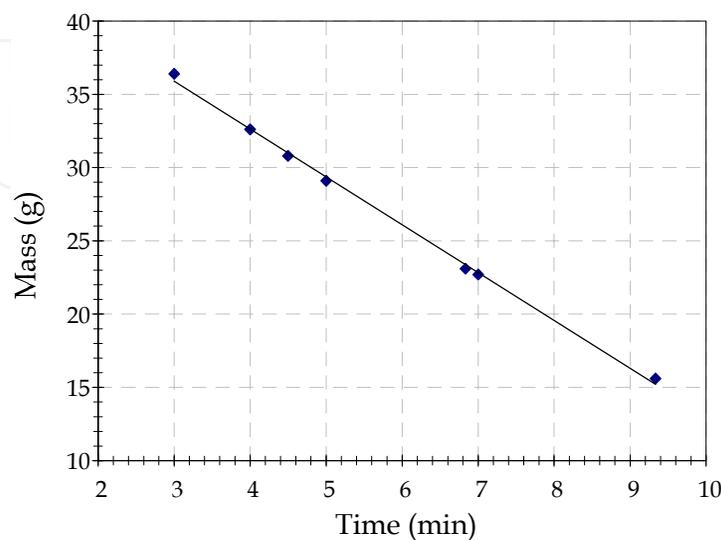


Fig. 8. Final internal mass experimental values approximation to a line.

| $\dot{m}_{eva}$ | -3.26829 | [g/min] |
|---|---|---|
| $b$ | 45.72 | [g] |
| $\sigma y$ | 0.32 | [g] |
| $\delta \dot{m}_{eva}$ | 0.06 | [g/min] |
| $\delta b$ | 0.35 | [g] |

Table 4. Evaporation rate $\dot{m}_{eva}$, intercept $b$, standard deviation $\sigma y$ and uncertainties in the estimated values of the evaporation rate $\delta \dot{m}_{eva}$ and intercept $\delta b$.

## 4.2 Temperature distribution on the outer surface of the thermosyphon tube

To study the temperature distribution along the thermosyphon, temperatures were recorded simultaneously at three points in the evaporator section, at one point in the adiabatic section and three more points in the condenser.

Figure 9 shows the temperature variation over time during the loading process. An applied power of 242 W and an ambient temperature of 20 °C were the test conditions. It was obtained a loading rate of 20% with a fluid excess of 5%. During the loading process may be present operation limits of the thermosyphon because this loading process is similar to the operation of a semi-open thermosyphon (Zhu et al., 2004).
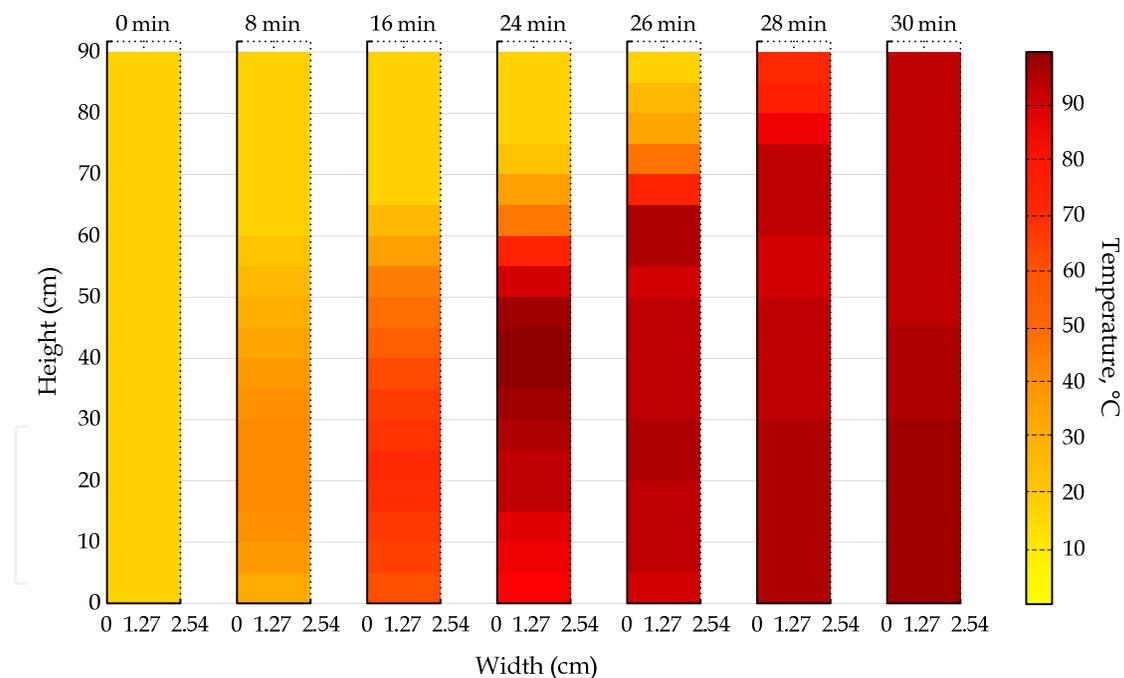


Fig. 9. Temperature rise versus time along the thermosyphon during loading.

## 4.3 Transported heat, efficiency and isothermal behavior

The data shown below were obtained in tests of thermosyphons loaded with five different rates. After the tests, from each thermosyphon was extracted and measured the amount of water contained in them in order to determine their loading rate. The obtained loading rates were: 28.82%, 24.81%, 18.91%, 15.06% and 10.17%.

From the results of this experiment can be extracted the heat transport capacity, efficiency and the temperature profile along the thermosyphons. Due to the restriction in the scope of this chapter there are presented below only the results for a cooling air mass flow of (0.38 kg/s).

Figure 10 shows the heat transported by the thermosyphons, loaded with different percentages of working fluid, with respect to operating temperature (thermocouple installed on adiabatic zone, $T_{ad}$). As shown in Figure 10, the thermosyphon with a load of 18.91% show the greatest amount of heat extracted in comparison to the rest of the thermosyphons. Therefore, in can be concluded that the thermosyphon loaded with this amount of fluid is the one that had a higher heat transfer for this flow of cooling air. On the other hand, the thermosyphons loaded with 28.82% and 10.17%, are the thermosyphons which have the lowest amounts of heat extracted.
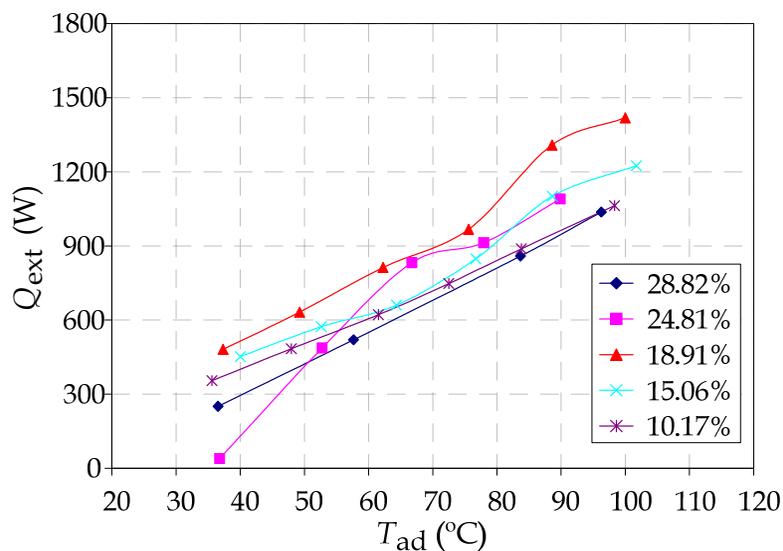


Fig. 10. Transported heat versus the operating temperature (cooling air flow: 0.38 kg/s).
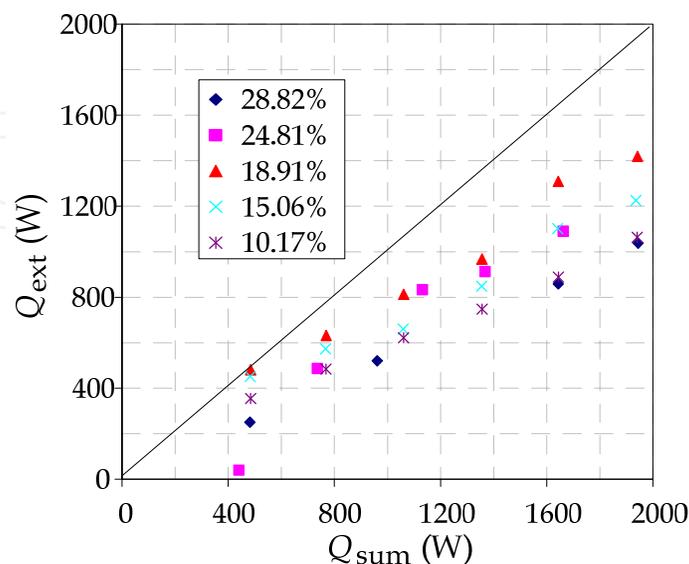


Fig. 11. Transported heat versus supplied heat (cooling air flow: 0.38 kg/s).

In Figure 11 it can be seen that as the heat flow supplied into the evaporation area increases, the ability to transfer heat of the thermosyphons decreases. Also, it can be seen in this plot that the thermosyphon loaded with 18.91% is the one that has a greater capacity to transport heat.
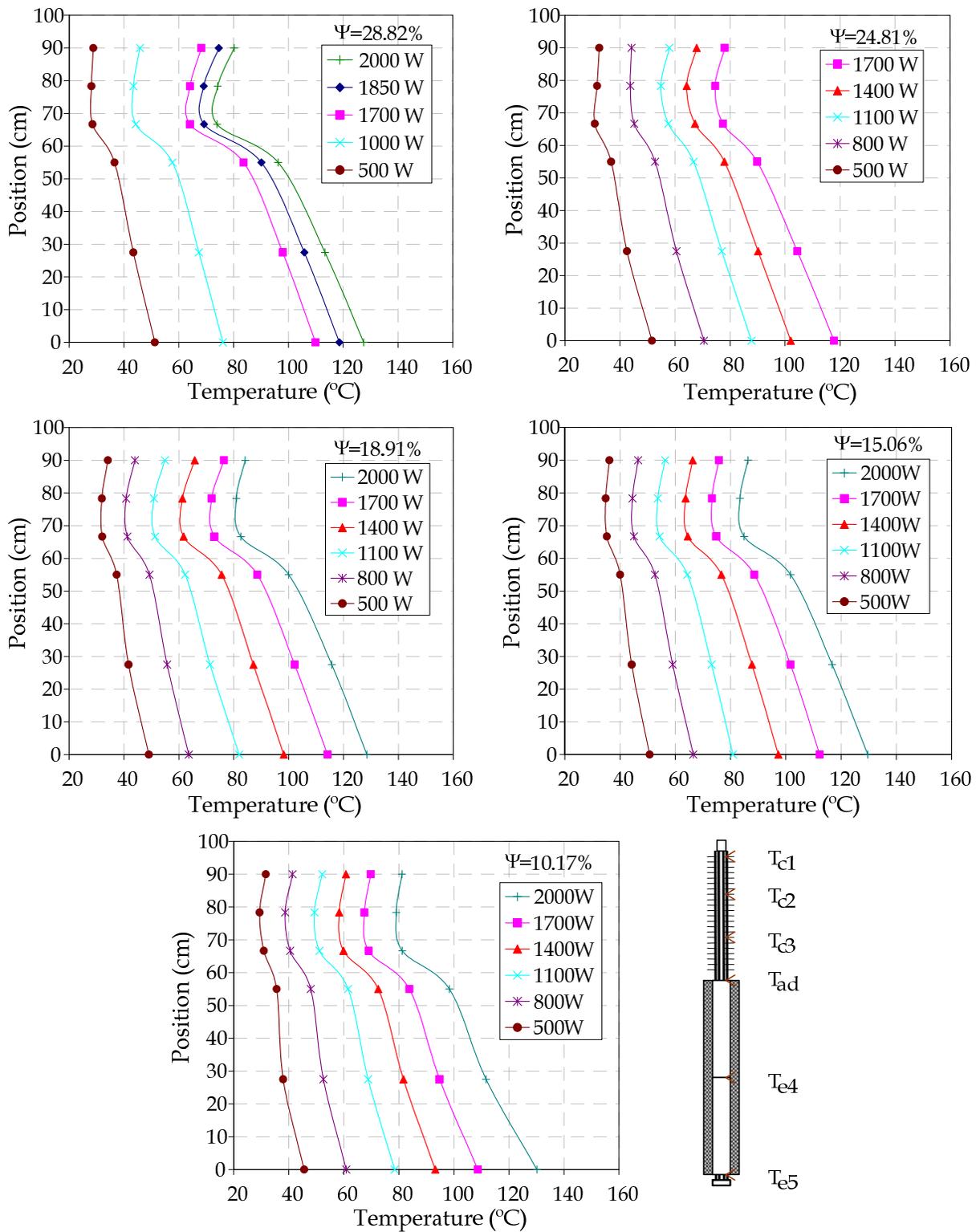


Fig. 12. Temperature profiles versus amounts of delivered heat (cooling air flow: 0.38 kg/s).

Figure 12 shows the temperature profiles along the thermosyphons for different loading rates. In the plots of Figure 12 it can be seen that profiles with higher temperatures are of the thermosyphons loaded with rates of 24.81%, 18.91% and 15.06%. This means that these thermosyphons reached higher temperatures, compared to the other two thermosyphons, under the same conditions of heat supply and cooling air flow. Moreover, these plots show that the lowest average temperature differences between condenser and evaporator are presented in the thermosyphon loaded with 10.17% in the range of heat input of 500 W to 800 W.

Also, it can be noted that for this thermosyphon it was presented a relative increase of temperature at the bottom of the evaporator for each value of the heat supplied, specifically for the heat supply 2000 W, this indicates the start of drying in the area of evaporation.

In the plots of Figure 12 it can be observed that at the top of the condenser (thermocouple $T_{c1}$) there is a higher temperature than in the middle of the condensation zone (low thermocouple $T_{c2}$). For this flow of cooling air, the rate of heat extraction is higher compared to the steam generation in the evaporator, so in this region drying occurs causing a rapid condensation on the top of the thermosyphon.

## 5. Conclusion

The methodologies for the calculation of three key parameters implemented in the design and manufacture of two-phase thermosyphons were developed. These key parameters are: the relationship of the lengths of evaporation and condensation zones, the operational pressure values and the evaporation rate of the working fluid during the filling process. The developed methodologies were applied in the design and manufacture of several two-phase thermosyphons. Distilled water was used as working fluid and hydrazine hydrate was added to it as corrosion inhibitor.

Two experimental installations were designed and constructed. One was used to load the thermosyphons, without using a vacuum pump, eliminating the non-condensing gases; the other one is a wind tunnel modified to test the performance of the thermosyphons using electrical resistances as heat source. A series of experiments to investigate the effect of parameters as heat power supply, amount of working fluid and speed of cooling air, on the performance of two-phase thermosyphons were carried out. In each experimental test, the temperature distribution along the external surface of thermosyphons, the heat power supply and the dissipated heat power by the device as well were registered. The results showed that the thermosyphons work isothermally with efficiencies around 90% for a working fluid loading of 20% of the internal volume of the thermosyphon.

The results of these investigations can be used to design and construct high efficiency two-phase thermosyphons for heat recovery from waste gas with a temperature up to 250 ºC.

## 6. Acknowledgment

## 7. Nomenclature

$A$ – area, [m$^2$];
$a$ – width of the gas-gas heat exchanger, [m];
$c_p$ – heat capacity at constant pressure, [J/kg K];
$d$ – diameter, [m];
$D$ – binary diffusion coefficient, [m$^2$/s];
$E$ – modulus of elasticity, [Pa];
Gr – Grashof number;
g – gravitational force, [m/s$^2$];
$H$ – specific enthalpy, [kJ/kg];

$\bar{h}$ – convective heat transfer coefficient, [W/m$^2$ K];

$\bar{h}_m$ – mass transfer coefficient, [m/s];
$I$ – electric current, [A];
$k$ – thermal conductivity, [W/m K];
$L_{eva}$ – characteristic length of evaporation, [m];
$l$ – length, [m];
$\dot{m}$ – mass flow, [kg/s];
$m$ – mass, [kg];
Nu – Nusselt number;
Pr – Prandtl number;
$p$ – pressure, [Pa];

$\dot{Q}$ – heat flow, [W]
$R$ – electric resistance, [Ω];
Ra – Rayleigh number;
$r$ – radius, [m];
$\zeta$ – stress, [N /m$^2$];
$S$ – entropy, [kJ/$^{\circ}$C]
$s$ – specific entropy, [kJ/kg $^{\circ}$C];
$T$ – temperature, [$^{\circ}$C, K];
$t$ – wall thickness of container, [m];
$U$ – voltaje, [V];
$u$ – specific internal energy, [kJ/kg];
$V$ – volumen, [m$^3$];
$v$ – velocity, [m/s];
x – quality;
$\Psi$ – loading rate;
$\alpha$ – thermal diffusivity, [m$^2$/s];
$\beta$ – volumetric thermal expansion coefficient, [K$^{-1}$];
$\nu$ – kinematic viscosity, [m$^2$/s];
$\rho$ – density, [kg/m$^3$].
$\upsilon$ – specific volume, [kg/m3];
$\phi$ – relative humidity;
Subscripts:
0 – normal conditions;
$a$ – air;

*eva* – evaporation;
*ext* – external;
f – working fluid;
*g* – hot gases;
*int* – internal;
*t* – total;
*w* – water.

## 8. References

Azada, E., Mohammadieha, F., & Moztarzadeh, F. (1985). Thermal performance of heat pipe heat recovery system. Journal of Heat Recovery Systems, Vol. 5, No. 6, pp. 561-570, ISSN 0890-4332.

Carvajal-Mariscal, I., Sanchez-Silva, F., Polupan, G., & Quinto-Diez, P. Additive amount influence on the thermal performance of a two-phase thermosyphon (IMECE2011-64177). *Proceedings of the ASME 2011 International Mechanical Engineering Congress & Exposition,* Denver Colorado, November 2011.

Faghri, A. (1995). *Heat pipe science and technology*, Taylor & Francis, ISBN 978-1560323839, New York USA.

Gershuni, A., Nishchik A., Pysmennyy Ye., Polupan G., Sanchez-Silva F., & Carvajal-Mariscal I. (2004). Heat exchangers of the gas-gas type based on finned heat pipes. *International Journal of Heat Exchangers,* Vol. 5, No. 2, pp. 347-358, ISSN 1524-5608.

Incropera, P. F., & Dewitt, P. D. (2006). *Introduction to Heat Transfer*, 5th edition, Prentice Hall, ISBN 978-0471457275.

Noie, S.H. (2005). Heat transfer characteristics of a two-phase closed thermosyphons. *Applied Thermal Engineering*, Vol. 25, No. 4, pp. 495-506, ISSN 1359-4311.

Park, J., Kang, K., & Kim, J. (2002). Heat transfer characteristics of a two-phase closed thermosyphon to the fill charge ratio. *International Journal of Heat and Mass Transfer*, Vol. 45, No. 23, pp. 4655-4661, ISSN 0017-9310.

Peterson, G.P. (1994). *An introduction to heat pipe modeling, testing, and applications*, John Wiley & Sons, Inc., ISBN 978-0471305125, New York USA.

Reay, D.A. (1981). A review of gas-gas heat recovery systems. Journal of Heat Recovery Systems, Vol. 1, No. 1, pp. 3-41, ISSN 0890-4332.

Terdtoon, P., Charoensawan, P., & Chaitep, S. (2001). Corrosion of tubes used in thermosyphon heat exchanger for waste heat recovery system: A case of internal Surface. *Heat Transfer Engineering*, Vol. 22, No. 4, pp. 18-27, ISSN 0145-7632.

Zhu, H., Wang, J., Zhang, Q., & Tu, C. (2004). Experimental study on transient behavior of semi-open two-phase thermosyphon. *Journal of Zhejiang University SCIENCE A*, Vol. 5, No. 12, pp. 1565-1569, ISSN 1673-565X.

Zuo, Z. J., & Faghri, A. (1998). A network thermodynamic analysis of the heat pipe. *International Journal of Heat and Mass Transfer*, Vol. 41, No. 11, pp. 1473-1484, ISSN 0017-9310.
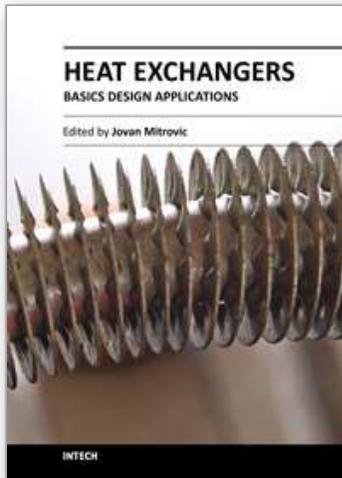
**Heat Exchangers - Basics Design Applications**

Edited by Dr. Jovan Mitrovic

Selecting and bringing together matter provided by specialists, this project offers comprehensive information on particular cases of heat exchangers. The selection was guided by actual and future demands of applied research and industry, mainly focusing on the efficient use and conversion energy in changing environment. Beside the questions of thermodynamic basics, the book addresses several important issues, such as conceptions, design, operations, fouling and cleaning of heat exchangers. It includes also storage of thermal energy and geothermal energy use, directly or by application of heat pumps. The contributions are thematically grouped in sections and the content of each section is introduced by summarising the main objectives of the encompassed chapters. The book is not necessarily intended to be an elementary source of the knowledge in the area it covers, but rather a mentor while pursuing detailed solutions of specific technical problems which face engineers and technicians engaged in research and development in the fields of heat transfer and heat exchangers.

**How to reference**

In order to correctly reference this scholarly work, feel free to copy and paste the following:

Ignacio Carvajal-Mariscal, Florencio Sanchez-Silva and Georgiy Polupan (2012). Development of High Efficiency Two-Phase Thermosyphons for Heat Recovery, Heat Exchangers - Basics Design Applications, Dr. Jovan Mitrovic (Ed.), ISBN: 978-953-51-0278-6, InTech, Available from: http://www.intechopen.com/books/heat-exchangers-basics-design-applications/development-of-high-efficency-two-phase-thermosyphons-for-heat-recovery

# INTECH
open science | open minds